for the crystalline spins, the $T_{1\rho}$ may be dominated by spin–spin interactions.[4,5] A more complete study is needed to determine the ratio of spin–lattice and spin–spin relaxation contributions to our $T_{1\rho}$ values, which we plan as soon as our instrument is modified for larger radiofrequency fields.

Motions, which in the amorphous region partly average out the chemical shift anisotropy, can also reduce the C–H cross-polarization efficiency for the amorphous line. This would explain the relative increase of the narrow amorphous line in the cross-polarization spectrum of the nonspinning sample with increasing cross-polarization time.

From the $T_{1\rho}$ measurement, one can estimate the percentage of crystallinity of the polymeric material. The $T_{1\rho}$ plots for every spinning frequency can be very accurately fitted with a function:

$$M(\tau) = A \exp(-\tau/t_1) + B \exp(-\tau/t_2)$$

where $M(\tau)$ is proportional to the ^{13}C signal after being spin locked for τ seconds, t_1 and t_2 represent the two $T_{1\rho}$ values to be determined, and A and B are the relative amounts of crystalline and amorphous material. We find a 70% (±5) crystalline and a 30% (±5) amorphous content. This is quite close to the value determined by X-ray diffraction, 63 and 37%, respectively. Even though our percentages depend somewhat on the length of the cross-polarization, they do provide strong support for the assignment that the long $T_{1\rho}$ is due to the amorphous component. For a more accurate determination of these percentages, one should take into account the difference of cross-polarization efficiencies for the amorphous and crystalline regions. We simply took the average for different spinning rates.

The spinning dependence of the crystalline $T_{1\rho}$ can in principle be explained by several mechanisms. A possible explanation could be, as suggested by Schaefer et al.,[3] that the anisotropy of $T_{1\rho}$ is averaged by the spinning, causing a shorter $T_{1\rho}$. However, preliminary studies on a nonspinning sample do not reveal such anisotropy. Also, the $T_{1\rho}$ plots of slow-spinning samples do not show a $T_{1\rho}$ dispersion except for the double-exponential decay.

Although there always remains the possibility that spinning modulates molecular motions and increases the spectral density at the rotating frame Larmor precession frequency, in our case, it seems likely that the spinning influences the spin–spin contribution to our $T_{1\rho}$. Further studies are in progress to explain this spinning dependence of $T_{1\rho}$.

The increase of the line width of the crystalline line at the highest spinning frequency may be related to the change of $T_{1\rho}$ with spinning. This line broadening might be explained as the result of strain in the material due to spinning forces and would only be observed at the high-spinning rates.

Conclusion

Poly(oxymethylene) (Delrin) consists of at least two components, one amorphous and at least one crystalline, having clearly different $T_{1\rho}$'s and different T_1's. If the difference we find in the $T_{1\rho}$'s of the crystalline and amorphous components of Delrin proves to be generally true for polymers, then such measurements will allow the determination of the degree of crystallinity in polymeric material. Also, this study shows that the T_1 of the crystalline component is very different from the amorphous T_1. Studying T_1, therefore, seems very worthwhile, especially because here spin–spin relaxation does not confuse the picture. T_1 measurements on Delrin will be reported later. Finally, the dependence of $T_{1\rho}$ and spectral width on spinning frequency needs further study.

Acknowledgment. We would like to thank Professor C. van Heerden, DSM, Geleen, for the X-ray determination of the Delrin crystallinity and Mr. J. W. M. van Os for his skilful assistance in the measurements. We thank the referees for their constructing criticism on the original manuscript. This work was carried out under the auspices of the Netherlands Foundation of Chemical Research (S.O.N.) and with the aid of the Netherlands Organization for the advancement of Pure Research (Z.W.O.).

References and Notes

(1) A. Pines, M. G. Gibby, and J. S. Waugh, *J. Chem. Phys.*, **59**, 569 (1973).
(2) J. Schaefer and E. O. Stejskal, *J. Am. Chem. Soc.*, **98**, 1031 (1976).
(3) J. Schaefer, E. O. Stejskal, and R. Buchdahl, *Macromolecules*, **10**, 384 (1977).
(4) E. O. Stejskal, J. Schaefer, and T. R. Steger, *Faraday Symp. Chem. Soc.*, in press.
(5) D. L. VanderHart and A. N. Garroway, to be published.
(6) To be published.
(7) Reported by E. M. Menger, *Faraday Symp. Chem. Soc.*, in press.
(8) A. N. Garroway, W. B. Moniz, and H. A. Resing, *Faraday Symp. Chem. Soc.*, in press.

Fluorescence Depolarization Study of the Glass–Rubber Relaxation in a Polyisoprene

J. P. Jarry* and L. Monnerie

Laboratoire de Physicochimie Structurale et Macromolêculaire, 75231 Paris, Cedex 05, France. *Received March 13, 1979*

ABSTRACT: The glass–rubber relaxation of an anionic poly(*cis*-1,4-isoprene) is investigated in the range of 10^{-7}–10^{-9} s, using a fluorescent label bonded within the chain backbones and several probes of varying size dissolved in the polymer matrix. Fluorescence depolarization allows appropriate models of rotational Brownian motion to be checked and relaxation times to be calculated as a function of temperature. Label and large probes are shown to reflect the glass–rubber relaxation in agreement with the WLF equation. The size dependence of the probe relaxation times is also analyzed. When the label and probe relaxation times are compared, the smallest chain segments involved in the glass–rubber relaxation seem to be composed of about five monomer units.

Fluorescence depolarization is a means of probing molecular rotational processes occurring in the range of 10^{-7}–10^{-10} s.[1-3] Fluorescence decay experiments give the autocorrelation function:[4-6]

0024-9297/79/2212-0927$01.00/0

$$M(t) = \left\langle \frac{3\cos^2\theta(t) - 1}{2} \right\rangle \quad (1)$$

where $\theta(t)$ is the angle between directions at time 0 and time t of the transition moment of a fluorescent molecule. Polarization measurements under continuous excitation yield the quantity:

$$\bar{M}(\tau) = \int_0^\infty M(t) \exp(-t/\tau)\, d(t/\tau) \quad (2)$$

where τ is the mean fluorescence lifetime ($\tau \simeq 10^{-8}$ s).

A number of experiments have been made on polymer solutions,[7,8,27] but very few are concerned with bulk polymers.[9] This paper presents an investigation of the glass–rubber relaxation in polyisoprene, using either one fluorescent label inserted in chain backbones or several probes dissolved in the polymer. Rotational relaxation times ranging from 10^{-7} to 10^{-9} s are measured as a function of temperature. The results are discussed in terms of the well-known WLF equation which is commonly used for mechanical relaxation data in a lower-frequency range ($f < 10^6$ Hz). The behavior of the fluorescent probes is compared to that of nitroxide spin probes reported by several authors[10-14] who studied the glass–rubber relaxation in the range of 10^{-7} s by the ESR technique. Moreover, additional information about the size of the segmental motions is shown to be available from a comparison of label and probes mobilities.

Materials

The commercially available polymer investigated is an anionic polyisoprene (Shell IR 307) of high molecular weight ($M_n \simeq 500\,000$) with high cis-1,4 configuration (92%). It was carefully purified by extraction with ethanol as a solvent and mixed with small amounts of dicumyl peroxide (Dicup) as a cross-linking agent. Samples were molded and cross-linked at 147 °C. Fluorescent label and probes were added as follows.

(a) The synthesis of labeled anionic polyisoprene chains is analogous to that reported previously for polystyrene.[15] Monofunctional "living" chains of molecular weight 300 000 are prepared and deactivated by 9,10-bis(bromomethyl)anthracene. The resultant chains of molecular weight 600 000 contain dimethylanthracene (DMA) fluorescent groups in their middle, as shown in Figure 1. Because the fluorescent transition moment lies along the chain axis, fluorescence depolarization will be insensitive to the rotation of the label around the 9,10 axis of the anthracene moiety and reflect only the motions of the backbone. The labeled polymer (1 g) and purified IR 307 polyisoprene (99 g) were mixed in solution before adding Dicup. The final concentration of DMA in bulk samples was 10^{-5} M.

(b) Four probes of varying size were employed: 9,10-dimethylanthracene (DMA) and three *trans*-diphenylpolyenes (DP). Their formulas and transition moments are shown in Table I. Cross-linked IR 307 samples were swollen with solutions of the probes in benzene and then dried in vacuo. The final probe concentration in bulk samples was approximately 2×10^{-5} M.

Methods

The mean fluorescence anisotropy[4,5]

$$\bar{r}(T) = (I_\parallel - I_\perp)/(I_\parallel + 2I_\perp)$$

was accurately measured under continuous illumination from −60 to +80 °C with an original instrument described elsewhere.[16] Values of the limit anisotropy[4,5] $r_0(25\ °C)$ and of the lifetime $\tau(25\ °C)$ were determined (see Table II)

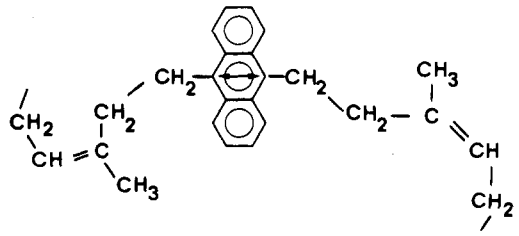

Figure 1. Position of the 9,10-dimethylanthracene (DMA) label in the middle of a chain skeleton. The double arrow indicates the direction of the transition moment.

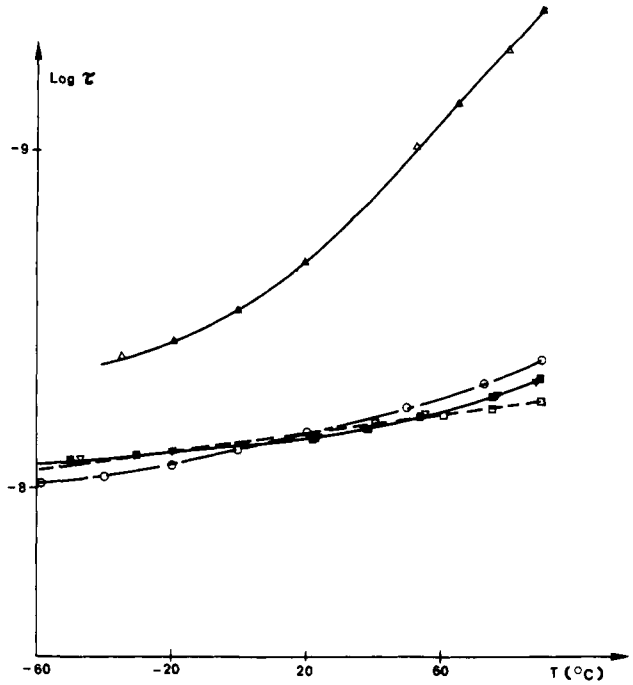

Figure 2. Lifetime τ vs. temperature for label (○) and probes: DPBD (△), DPHT (■), DPOT (▽), DMA (□).

Table I
Formulas, Approximative Lengths (Å), and Transition Moments (Double Arrows) of the Probes DMA, DPBD, DPHT, and DPOT[a]

DMA 6.5 Å	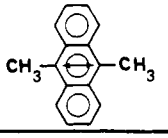
DPBD 11.5 Å	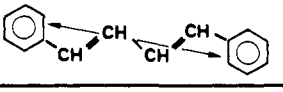
DPHT 14 Å	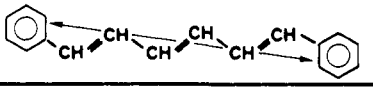
DPOT 16.5 Å	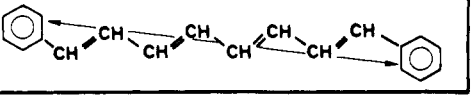

[a] DMA, 9,10-dimethylanthracene; DPBD, 1,4-diphenylbutadiene; DPHT, 1,6-diphenylhexatriene; DPOT, 1,8-diphenyloctatetraene.

from fluorescence decay experiments at room temperature, using equipment and methods reported previously.[17] Since the value $r_0(25\ °C)$ was found to be nearly identical with $\bar{r}$ at low temperature, it was reasonable to assume r_0 to be independent of temperature. The decrease of τ with increasing temperature was derived from measurements

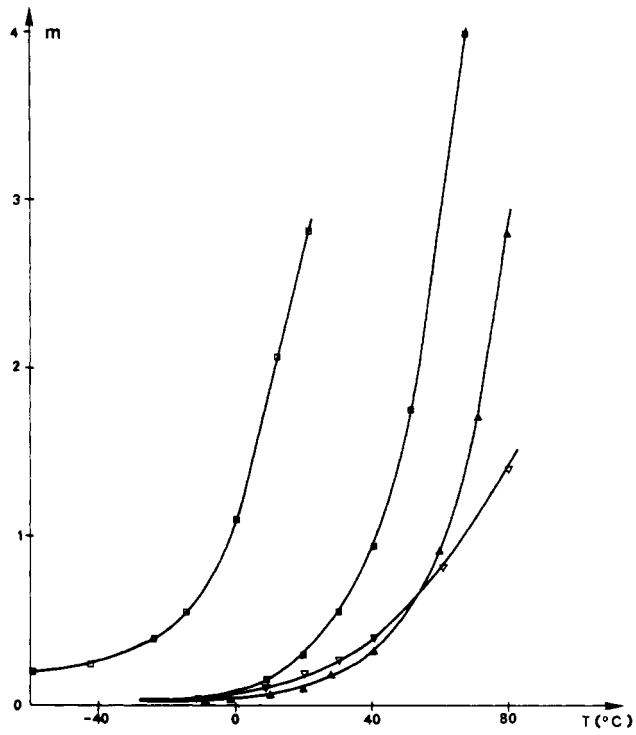

Figure 3. Mobility parameter m vs. temperature for the four probes: DPBD (▽), DPHT (■), DPOT) (▲), DMA (□).

of the total fluorescence intensity under continuous excitation (see Figure 2).

From $\bar{M}(T)$ defined by eq 2 and calculated by

$$\bar{M}(\tau(T),T) = \bar{r}(T)/r_0$$

we got the mobility parameter m:

$$m = \bar{M}^{-1} - 1$$

which increases from zero (molecular relaxation times much larger than the lifetime) to infinity (relaxation times much smaller than the lifetime). Relaxation times were derived from $m(T)$ and $\tau(T)$ by using a model of Brownian rotational motion. Two models have proved convenient. The well-known Einstein–Stokes model for a spherical body predicts a monoexponential autocorrelation function:

$$M(t) = \exp(-t/\tau_R) \tag{3}$$

where τ_R is a unique relaxation time which is simply obtained from:

$$\log \tau_R = \log \tau - \log m \tag{4}$$

A more specific model of chain dynamics[18] assumes segmental motions resulting in diffusive propagation of the segmental orientations along the chain backbones. This model can be considered as a version of the usual Rouse model in which translational coordinates have been replaced by angular ones, to account for rotational motions. Accordingly, the autocorrelation function is expressed as:

$$M(t) = \exp(t/\rho)\ \mathrm{erfc}(t/\rho)^{1/2} \tag{5}$$

where the characteristic time ρ is inversely proportional to the frequency of the motions and is given by:

$$\log \rho = \log \tau - \tfrac{1}{2} \log m \tag{6}$$

Finally, the temperature dependence of $\log \tau_R$ or $\log \rho$ was compared to the WLF equation:[19]

$$\log a_T = \log \tau_R \text{ (or } \log \rho) + \text{constant}$$

$$\log a_T = -\frac{A(T - T_g)}{B + T - T_g} \tag{7}$$

where $T_g = -60$ °C is the ATD glass-transition temperature of the IR 307 polyisoprene, and A and B are two constants, the values of which are assumed identical with those of the poly(*cis*-1,4-isoprene) studied by Ferry[20] ($A = 16$ and $B = 57$).

Results

Probes. It is apparent from the plots of m vs. temperature shown in Figure 3 that the behavior of the three DP probes is quite different from that of DMA. The rotational mobility of the DP probes appears to reflect the glass–rubber relaxation. The onset of mobility occurs at about −10 °C, that is 50 °C above the usual T_g. This shift illustrates the time–temperature superposition principle:[19] the higher the frequency of the experimental technique, the higher the temperature at which the transition is observed. On the other hand, the smaller DMA probe exhibits a higher mobility which vanishes below −60 °C and cannot be related to the glass–rubber relaxation.

A quite similar probe size effect has been reported in several papers[10-13] based on the ESR spin-probe method. As suggested by Kumler and Boyer,[13] the dynamic behavior of a particular probe depends on its relative size compared to that of the moving polymer segments involved in the glass–rubber relaxation. If the probe is larger than a critical size v^*, its mobility is modulated by the same free volume fluctuations as the polymer segments, and it is "seeing" the glass transition. Probes smaller than v^* start to move below T_g, and their mobility may be related to secondary relaxations. Moreover, Kumler and Boyer[21] showed that v^* could be conveniently identified with the activation volume Δv calculated from the Eby formula. For polyisoprene, they reported a value of $\Delta v = 160$ cm^3/mol, which corresponds to a sphere of 8-Å diameter. Accordingly, the DP probes, whose lengths range from 11.5 to 16 Å, respond to the glass–rubber relaxation, while the 6.5 Å long DMA probe does not. This accordance between fluorescent and spin probes lends additional support to the proposition that the dynamic behavior of a guest molecule mainly depends on its size.

For the four probes, fluorescence decay experiments at room temperature show that $M(t)$ is remarkably monoexponential and that the simple Einstein–Stokes model is valid.[22] The relaxation times τ_R can be calculated from eq 4 as a function of temperature. As shown in Figure 4, the slopes of $\log \tau_R$ for the three DP probes are in good agreement with that of $\log a_T$ calculated by eq 7. These large probes obey the WLF equation. Their relaxation times correspond to the rotation of their symmetry axis about a direction perpendicular to it, since it is known that both absorption and emission transition moments lie along this axis.[23] Assuming the Perrin theory for prolate ellipsoids,[24] we obtain:

$$\tau_R = \frac{8\pi\eta}{9kT} a^3 \left(2 \ln \frac{2a}{b} - 1\right)^{-1} \tag{8}$$

where a and b ($b < a$) are the axes of the ellipsoid and where $\eta(T)$ is the local viscosity which describes the local friction acting on the probe molecules. As is shown in Figure 5, the length dependence of the probe relaxation times is fairly well described by eq 8. Finally, this equation accounts for both size and temperature effects, the ratio $\eta(T)/T$ being proportional to a_T in the WLF theory.

This holds only for probes larger than the critical size v^*. The small DMA probe does not obey the WLF

Table II
Limit Anisotropies r_0 and Lifetimes τ at 25 °C[a]

	label	probes			
	DMA	DMA	DPBD	DPHT	DPOT
r_0(25 °C)	0.24	0.24	0.31	0.32	0.32
τ(25 °C)	8 ns	7 ns	2 ns	7 ns	7 ns

[a] Accuracies: $\Delta r_0/r_0 = 2 \times 10^{-2}$, $\Delta\tau/\tau = 10^{-2}$.

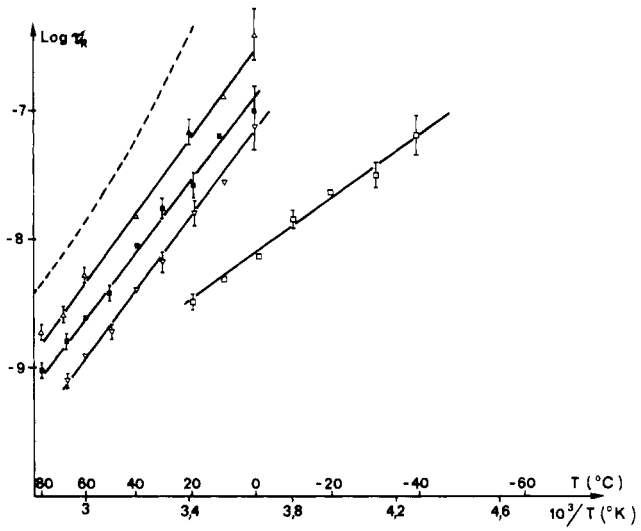

Figure 4. Logarithmic plot of τ_R vs. $1/T$ for the four probes in uncross-linked polymer: DPBD (▽), DPHT (■), DPOT (△), DMA (□). The dotted line represents log a_T + 3, calculated from eq 7.

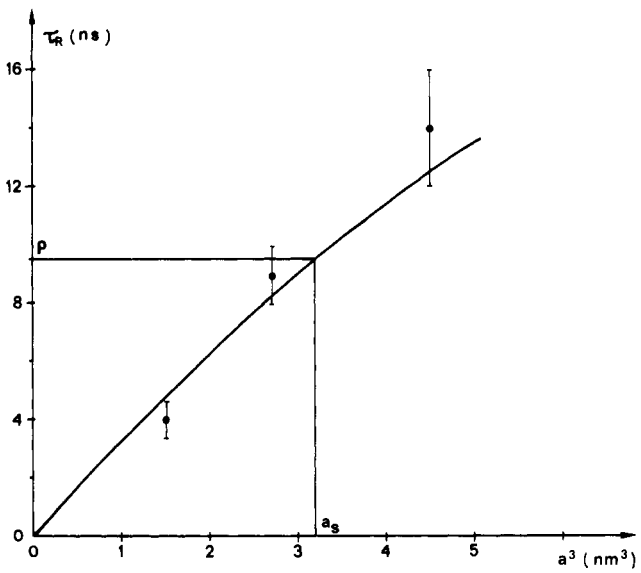

Figure 5. Relaxation times τ_R of the DP probes at 40 °C vs. length a. The curve represents eq 8 with b = 2.5 Å and η = 0.15 P. ρ and a_S correspond to the label.

equation (see Figure 4). From the slope of d log τ_R/dT, an activation energy of E_a = 6.5 kcal mol^{-1} can be obtained, which is about half of that of the DP probes. This behavior is perhaps related to a secondary transition of polyisoprene. Extrapolating the curve log τ_R vs. T, this transition would appear around 110 K at 1 Hz or 125 K at 20 Hz. This extrapolation may agree with the mechanical data reported by Morgan et al.,[28] who found two weak maxima of the loss tangent for T = 100 and 130 K at frequencies close to 20 Hz. Unfortunately, they did not measure the corresponding activation energies which would allow us to

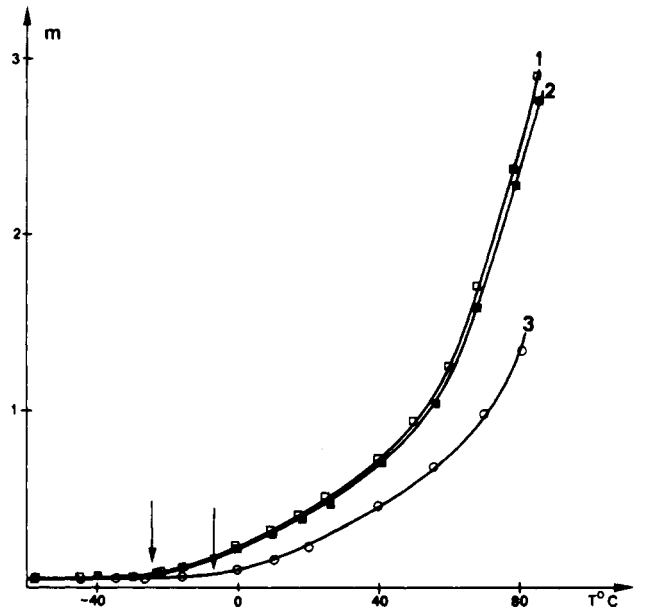

Figure 6. Mobility parameter m of the label vs. temperature for various cross-linking densities. As usual, the mean molecular weight M_c between cross-links was determined from maximum swelling ratio: uncross-linked (T_g = −59 °C) (□); $M_c = 4 \times 10^4$ (T_g = −59 °C) (■); $M_c = 0.7 \times 10^4$ (T_g = −54 °C) (○).

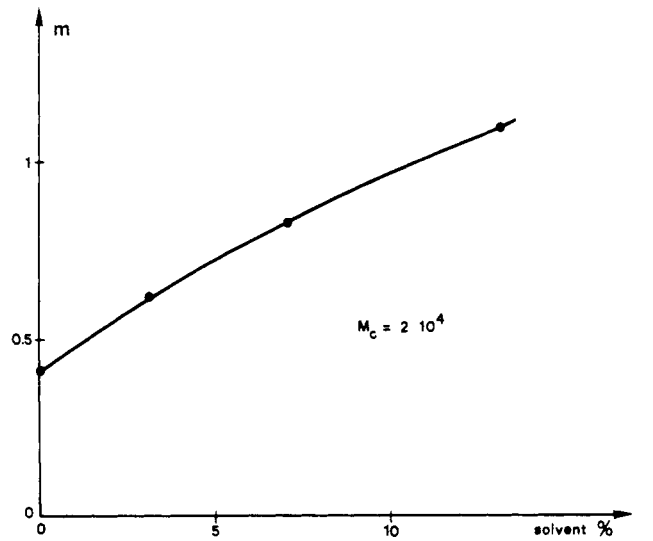

Figure 7. Mobility parameter m of the label vs. volume fraction of solvent (toluene) at 25 °C, $M_c = 2 \times 10^4$.

confirm a possible relationship between these low-temperature mechanical transitions and the rotational motion of the DMA probe.

Label. Although small, the chemically bonded DMA label reflects the glass–rubber relaxation. The mobility parameter m is plotted vs. temperature in Figure 6, for dry networks of low cross-linking density. The curves are similar to that of the DP probes. If the cross-linking density is increased, both the usual T_g and the onset of label mobility are shifted toward higher temperatures. Moreover, the mobility is increased by swelling (see Figure 7), in accordance with the fact that T_g is lowered by addition of small organic molecules.

Contrary to the case of probes, the fluorescence decay experiment is difficult to analyze for the DMA label, because of the complicated form of the total intensity ($I_\parallel$ + $2I_\perp$) decay. It is however possible to assert that $M(t)$ is not a single exponential and that the Einstein–Stokes model does not hold. Besides, this model would lead to

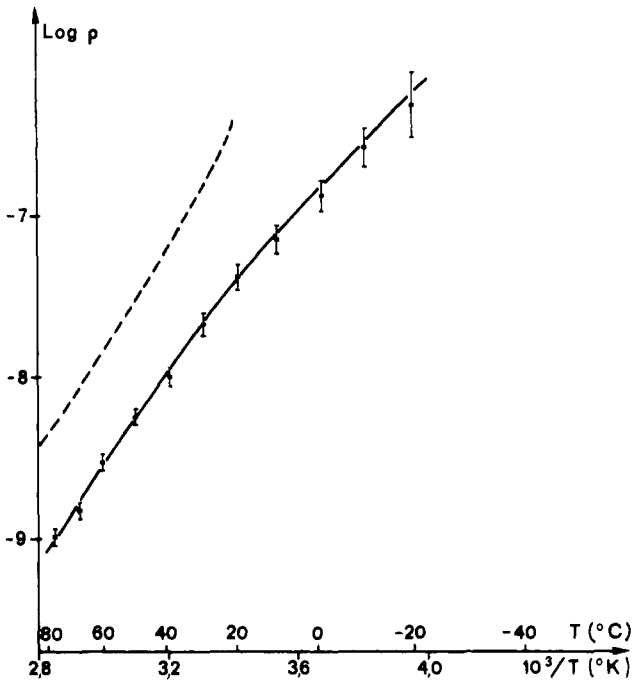

Figure 8. log ρ vs. temperature for DMA label in uncross-linked polymer. The dotted line corresponds to log a_T + 3, calculated from eq 7.

a strong discrepancy between the slopes of log τ_R calculated by eq 4 and log a_T. On the contrary, the model assuming orientational diffusion along the chain backbones gives a rather good agreement between +20 and +80 °C. As is shown in Figure 8, the slopes of log a_T and of log ρ calculated by eq 6 are quite close in this temperature range.

However, in the low mobility range lying between −10 and +20 °C, the slope of log ρ is smaller than that predicted by the WLF equation, indicating a lower apparent activation energy. This disagreement could be due (i) either to the failure of the diffusion model (as it is known that the Rouse model fails in the low-temperature part of the mechanical glass transition) (ii) or to the occurrence of a secondary transition which could prevail over the primary glass transition in this temperature range where the glass–rubber relaxation times are still larger than the fluorescence lifetime and where primary and secondary relaxations could merge[29] in the frequency–temperature map. It should be noted that similar slope changes of log τ vs. T^{-1} have been reported for both fluorescent[30] and spin[31] probes.

Further information can be obtained by comparing label and probe mobilities. The glass–rubber relaxation very likely involves several types of chain segments of varying sizes and relaxation times. Since the autocorrelation $M(t)$ is most sensitive to the smallest relaxation times, the characteristic time ρ of the DMA label principally describes the smallest segment motions. On the basis of the free-volume theory, the mobility of molecular species is mainly dependent on their size, and the length a_S of the smallest segments should be comparable to that of a probe, the relaxation time of which equals ρ. One obtains $a_s \simeq 14$ Å by using the relation $\tau_R(a)$ of the DP probes (see Figure 5). From earlier configurational studies of polyisoprene by Abe and Flory,[25] such a length represents about five monomers in average conformation.

Conclusion

In this first fluorescence depolarization study of the glass–rubber relaxation, the use of labels and large probes has been shown to afford useful information about the nature and size of the involved segmental motions. The validity of the WLF equation is extended to the unusually short time range of 10^{-7}–10^{-9} s. The rotational motion of the label seems to involve diffusional processes along the chains. Moreover, the smallest moving chain segments are estimated to contain about five monomer units by comparing the label relaxation time ρ with the size-dependent probe relaxation times $\tau_R(a)$. This rather high value might explain the disagreement between ^{13}C NMR and fluorescence depolarization results. In a recent study of natural rubber (usual T_g = −70 °C), Schaefer[26] showed that a very broad distribution of relaxation times was neceassary to account for measurements of T_1, T_2, and NOEF. He found a mean value $\bar{\tau} = 4 \times 10^{-10}$ s at T = 40 °C (i.e., $T = T_g$ + 110 °C). This is about one decade smaller than the value $\rho_{FD} = 5 \times 10^{-9}$ s derived from fluorescence depolarization for IR 307 polyisoprene (usual T'_g = −60 °C) at the equivalent temperature T' = 50 °C (i.e., $T' = T'_g$ + 110 °C). NMR experiments akin to those reported by Schaefer have been carried out in our laboratory for IR 307 polyisoprene between 30 and 100 °C. They confirm Schaefer's results and yield and apparent activation energy E_{NMR} = 7.8 kcal/mol. Since the glass–rubber relaxation seems to involve several monomer units, as observed by fluorescence depolarization, it is suggested that the NMR technique is sensitive to more local and faster molecular motions. This is consistent with the fact that E_{NMR} is substantially smaller than the apparent activation energy E_{FD} = 12 kcal/mol for the label and large probes.

Acknowledgment. The authors wish to thank Dr. J. Brossas for assistance with the synthesis of labeled polymer and Drs. B. Valeur and F. Laupretre, who performed the fluorescence decay and NMR experiments.

References and Notes

(1) Perrin, F. *Ann. Phys. (Paris)* **1929**, *12*, 169.
(2) Weber, G., *Biochem. J.* **1952**, *51*, 155.
(3) Wahl, Ph. *J. Polym. Sci.* **1958**, *29*, 375.
(4) Jablonski, A. *Z. Naturforsch., A* **1961**, *16*, 1.
(5) Gordon, R. G. *J. Chem. Phys.* **1966**, *45*, 1643.
(6) Tao, T. *Biopolymers* **1969**, *8*, 609.
(7) Anufriera, Ye. V.; Gotlib, Yu. Ya.; Krakoviak, M. G.; Skorokhodov, S. S. *Vysokomol. Soedin., Ser. A* **1972**, *14*, 1430.
(8) Nishijima, Y. *J. Macromol. Sci., Phys.* **1973**, *8*, 389.
(9) Chapoy, L. L. *Chem. Scr.* **1972**, *2*, 35.
(10) Rabold, G. P. *J. Polym. Sci., Part A-1* **1969**, *7*, 1203.
(11) Gross, S. C. *J. Polym. Sci., Part A-1* **1971**, *9*, 3327.
(12) Kumler, P. L.; Boyer, R. F. *Macromolecules* **1976**, *9*, 903.
(13) Kumler, P. L.; Keinath, S. E.; Boyer, R. F. *Polym. Prepr., Am. Chem. Soc., Div. Polym. Chem.* **1976**, *17*, 28.
(14) Kovarskii, A. L.; Vasserman, A. M.; Buchachenko, A. L. *Vysokomol. Soedin., Ser. A* **1971**, *13*, 1647.
(15) Valeur, B.; Rempp, P.; Monnerie, L. *C. R. Hebd. Seance Acad. Sci., Ser. C* **1974**, *279*, 1009.
(16) Jarry, J. P.; Sergot, Ph.; Pambrun, C.; Monnerie, L. *J. Phys. E* **1978**, *11*, 702.
(17) Valeur, B.; Monnerie, L. *J. Polym. Sci., Polym. Phys. Ed.* **1976**, *14*, 11.
(18) Valeur, B.; Jarry, J. P.; Gény, F.; Monnerie, L. *J. Polym. Sci., Polym. Phys. Ed.* **1975**, *13*, 667.
(19) Ferry, J. D. "Viscoelastic Properties of Polymers", 2nd ed.; Wiley: New York, 1970.
(20) Shen, S. P.; Ferry, J. D. *Macromolecules* **1968**, *1*, 270.
(21) Boyer, R. F.; Kumler, P. L. *Macromolecules* **1977**, *10*, 461.
(22) The diphenylpolyenes are markedly nonspherical, and their whole mobility should be represented by a diffusion tensor. However, their fluorescent transition moment lies along a symmetry axis, so that the rotation of this moment is only determined by one component of the tensor.
(23) Cehelnik, E. D.; Cundall, R. B.; Timmons, C. J.; Bowley, R. M., *Proc. R. Soc. London, Ser. A* **1973**, *335*, 387.
(24) Perrin, F. *J. Phys. Radium* **1934**, *5*, 497.
(25) Abe, Y.; Flory, R. J. *Rubber Chem. Technol.* **1972**, *45*, 982.

(26) Schaefer, J. *Macromolecules* **1973**, *6*, 882.
(27) Valeur, B.; Monnerie, L. *J. Polym. Sci., Polym. Phys. Ed.* **1976**, *14*, 11.
(28) Morgan, R. J.; Nielsen, L. E.; Buchdahl, R. *J. Appl. Phys.* **1971**, *42*, 4653.
(29) Weber, G.; Tormala, P. *Colloid Polym. Sci.* **1978**, 256, 638.
(30) Ueno, H.; Otsuka, S.; Kushimoto, A. *Kobunshi Ronbunshu* **1978**, *35*, 339.
(31) Smith, P. M.; Boyer, R. F.; Kumler, P. L. *Macromolecules* **1979**, *12*, 61.

Polymeric Materials from the Gel State. The Development of Fringed Micelle Structure in a Glass

Steve Wellinghoff,* Julie Shaw, and Eric Baer

Department of Macromolecular Science, Case Western Reserve University, Cleveland, Ohio 44106. *Received December 26, 1979*

ABSTRACT: Rapid cooling of concentrated solutions of atactic (APS) and isotactic (IPS) polystyrene and poly(2,6-dimethylphenylene oxide) in low molecular weight solvents yields gels which are cross-linked by small 20–100 Å fringed micelle crystallites and/or glassy microdomains. The crystal size and perfection and microphase separation in glasses of PS, PPO, and their blends cast from gel solution are affected by the gelation solvent and annealing treatement. The IPS gel crystals consist of a high-energy conformational variant of the usual isotactic configuration, while the normal 4_1 helical tetragonal form of PPO was found for its gel crystals. These gel glasses are useful for exploring, in a controlled way, the effect of microheterogeneity on localized plastic deformation.

The region below the binodal in the phase diagram of a two-phase system exhibiting an upper critical solution temperature (UCST) can be divided into two parts, namely, a metastable region between the binodal and the spinodal and an unstable region below the spinodal.[1] In the metastable region, minimization of the free energy of the system requires that large excursions in concentrations about the average occur in neighboring regions. The large composition difference that exists across the phase interface is responsible for a relatively large surface free energy. Thus, in this region, phase separation is reminiscent of crystal nucleation and growth, and isolated particles will nucleate and continue to grow at the same internal composition until they are large enough to scatter light. Typically, polymer solutions will exhibit this type of behavior near the Θ temperature.

If the mobility of the system is sufficiently low and if the solution is quenched rapidly to a temperature below the spinodal line, nucleation and growth can be avoided, and the solution can phase separate by a spinodal mechanism. Since within this region the curvature of the free energy of the system with respect to composition is negative, even infinitesimal concentration fluctuations will continue to grow. Provided that the volume fraction of the minor component is high enough, the microphase morphology will consist of two continuous interconnected phases separated by a characteristic distance. In the initial stages of microphase separation, the same characteristic interphase distance will be maintained as the two phases diverge in composition with increasing time. If one of the phases is a polymer-rich phase, the morphology will be frozen in as soon as the polymer concentration increases enough to cause the T_g of this phase to be below the temperature of phase separation. Macroscopically, this system will exhibit rubbery, gelatinous characteristics as a consequence of the low mobility within the interconnected polymer-rich phase.

Concentrated (>5–10%) solutions of APS in decalin will phase separate into opaque gels at ca. 10 °C;[2] turbid, freely-flowing solutions develop at lower concentrations. The polystyrene self-associations that promulgate phase separation do not appear suddenly at the CST. Shear flow experiments can detect these associations at temperatures as high as 40 °C in decalin solutions which are quite clear.[3]

If the polymer is crystallizable, the concentration gradients that occur in the neighborhood of the CST will often be sufficient to induce polymer crystallization. In the case of spinodal phase separation, the crystallites that form in the polymer-rich phase can immobolize polymer chains in the network and stabilize the phase separation at a domain size below that required for the scattering of visible light. For example, isotactic PS (IPS)–decalin solutions form clear gels at <15 °C,[4] quite close to the UCST of 10 °C. Cross-links composed of 100-Å fringed micelle crystals were found to be responsible for the rubbery behavior of the solution. Paul[5] has summarized many other polymer–solvent systems that undergo the phenomenon of thermally reversible gelation. The observed decrease in melting point of the gel as the difference between the Hildebrand solubility parameters of the polymer and solvent decreased led him to suggest that gelation might be predicted by a thermodynamic theory of phase separation provided that surface energy contributions arising from the very small sizes of the phase were taken into account.

We were interested in these gel systems because they provided a route for making glassy polymer films containing well-defined crystalline heterogeneities of ca. 100 Å in size. These would be formed in a spinodally-phase-separating system of constant interphase distance. Heterogeneities of this dimension are thought to have a profound influence on the development of localized plastic deformation.[6] In addition, this glass morphology clearly avoids the complicated structure-property correlations that would attend a spherulitic structure and minimizes the uncertainty in heterogeneity that would otherwise exist in a completely amorphous glass. This paper concentrates on the preparation and structural characterization of polystyrene (PS), poly(2,6-dimethylphenylene oxide) (PPO), and PS–PPO glasses cast from gelled solutions. A subsequent report will discuss the plastic deformation behavior of these materials and its relationship to the heterogeneities introduced into the glass.

Experimental Section

Additive-free PPO ($M_v \simeq 25\,000$; General Electric Co.), narrow-fraction, atactic polystyrenes (APS's) (M_n = 4000, 37 000,

0024-9297/79/2212-0932$01.00/0